Title

The microtubule depolymerising agent CYT997 causes extensive ablation of tumor vasculature in vivo[#]

Authors

Christopher J. Burns, Emmanuelle Fantino, Andrew K. Powell, Steven D. Shnyder, Patricia A. Cooper, Stuart Nelson, Christopher Christophi, Cathy Malcontenti-Wilson, Valentina Dubljevic, Michael F. Harte, Max Joffe, Ian D. Phillips, David Segal, Andrew F. Wilks, Gregg D. Smith

Affiliation

YM BioSciences Australia, Frankston, VIC, 3199, Australia (CJB, EF, AKP, VD, MFH, MJ, IDP, DS, RF, AFW, GDS).

Institute of Cancer Therapeutics, University of Bradford, Richmond Road, Bradford, West Yorkshire, BD7 1DP, UK (SDS, PAC, SN).

Department of Surgery, The University of Melbourne, Austin Health, Heidelberg, VIC, 3084, Australia (CC, CM-W).

Running Title: CYT997 causes ablation of tumor vasculature in vivo

Corresponding Author: Dr Christopher J. Burns

YM BioSciences Australia

PO Box 11194

Frankston

VIC 3199

Australia

Phone: +61 0 401 090 226

Fax: + 61 3 9787 7534

Email: cburns@ymbiosciences.com.au

Text Pages:

Figures: 5 (and one supplementary figure)

References: 40

Words in Abstract: 228

Words in Introduction: 490

Words in Discussion: 1267

List of non-standard abbreviations: VDA, vascular disrupting agent; HUVEC, human umbilical vein endothelial cells; CA4P, combretastatin A-4P; VEGF, Vascular endothelial growth factor.

Section assignment: Chemotherapy, Antibiotics, and Gene Therapy

JPET Fast Forward. Published on September 14, 2011 as DOI: 10.1124/jpet.111.186965
This article has not been copyedited and formatted. The final version may differ from this version.

Abstract

The orally active microtubule disrupting agent CYT997, previously reported by us, is potently cytotoxic to a variety of cancer cell lines in vitro and shows anti-tumor activity in vivo. In addition to its cytotoxic activity, CYT997 possesses antivascular effects on tumor vasculature. To further characterise the vascular disrupting activity of CYT997 in terms of dose and temporal effects, we studied the activity of the compound on endothelial cells in vitro and on tumor blood flow in vivo using a variety of techniques. In vitro, CYT997 is shown to potently inhibit proliferation of VEGF stimulated HUVEC cells (IC_{50} 3.7 ± 1.8 nM) and to cause significant morphological changes at 100 nM including membrane blebbing. Using the method of corrosion casting visualised with scanning electron microscopy, a single dose of CYT997 (7.5mg/kg, i.p.) in a metastatic cancer model is shown to cause destruction of tumor microvasculature in metastatic lesions. Furthermore, repeat dosing of CYT997 at 10 mg/kg and above (i.p., b.i.d.) is shown to effectively inhibit development of liver metastases. The time and dose-dependence of the anti-vascular effects is studied in a DLD-1 colon adenocarcinoma xenograft model using the fluorescent dye Hoechst 33342. CYT997 demonstrates rapid and dose-dependent vascular shutdown which persists for greater than 24 h after a single oral dose. Together the data demonstrate that CYT997 possesses potent anti-vascular activity and supports continuing development of this promising compound.

Introduction

Drugs that disrupt the cellular microtubule network are some of the most successful anticancer agents developed to date, emphasizing the fundamental role microtubules play in cell division, organelle transport, morphology and motility. Perturbation of normal microtubule dynamics through the binding of drugs to the protein subunits of microtubules, α- and β-tubulin, or their associated proteins, leads to blockade of the cell cycle at the G2/M boundary and ultimately to cell death through apoptotic or non-apoptotic processes (Honore *et al*, 2005).

Drugs of the *Taxane* and *Vinca* class, which target separate sites on the α, β-tubulin dimer and cause microtubule polymerisation and depolymerisation, respectively, are currently first-line therapy for many cancers (Hamel, 1996). Nonetheless, these agents have drawbacks including the development of resistance during the course of their use (van Ark-Otte *et* al, 1998; Yin *et al*, 2007), and the necessity for intravenous administration due to their limited oral bioavailability. As such there has been considerable effort in recent years in the discovery and development of novel tubulin binding drugs which possess improved physicochemical and pharmacokinetic properties, thereby allowing for oral administration (Hearn *et al*, 2007).

Of the numerous examples of novel small molecule tubulin binding compounds, a selected few have been shown to possess effects on tumor vasculature in *in vivo* models and in clinical trials (Schwartz, 2009). For example, the phosphate ester pro-drug of combretastatin A-4P (CA4P, Zybrestat™) was found to induce a rapid reduction in tumor blood flow and a concomitant increase of cellular necrosis in mouse tumor models (Malcontenti-Wilson *et al*, 2001). Now known as Vascular Disrupting Agents (VDAs), several drug candidates with this mechanism of action have entered clinical development, and there is encouraging evidence that the

approach may be useful in the treatment of solid tumors (Tozer *et al*, 2005a). Other tubulin binding agents that have been tested in the clinic with reported vascular disrupting activity include ABT-751 (Luo *et al*, 2009), AVE8062 (Hori and Sato, 2004) and NPI-2358 (Nicholson *et al*, 2006). All these drugs inhibit tubulin polymerisation and have been shown to possess anti-vascular effects in various *in vitro* and *in vivo* models.

We have previously reported the discovery (Burns *et al*, 2009a) and preliminary biological characterisation (Burns *et al*, 2009b) of CYT997, a novel synthetic microtubule depolymerising compound first synthesised in our laboratories. The compound inhibits the polymerisation of tubulin with an IC_{50} of ~3 μM, and possesses potent cytotoxic activity against a panel of cancer cell lines. Importantly, CYT997 is orally bioavailable and shows significant activity in tumor xenograft models when dosed orally. Antivascular activity of the compound was demonstrated *in vitro* against human umbilical vein endothelial cells (HUVECs), and *in vivo*, where a significant reduction in tumor blood flow was observed after both i.p. and p.o. dosing. In this paper, we further characterise the antivascular effects of CYT997 *in vitro* and *in vivo* as well as report the dose effects and pharmacodynamic effect of the compound in a xenograft model.

Materials and Methods

CYT997 ((*S*)-1-ethyl-3-(2-methoxy-4-(5-methyl-4-((1-(pyridin-3-yl)butyl)amino)pyrimidin-2-yl)phenyl)urea) was prepared as previously described (Burns *et al*, 2009a) as was CA4P (phosphate prodrug of (Z)-2-methoxy-5-(3,4,5-trimethoxystyryl)phenol) (Pettit *et al*, 2005). Vincristine, paclitaxel and doxorubicin were purchased from Sigma (St. Louis, WI, USA). HUVEC cells were obtained from

Invitrogen (Mulgrave, VIC, Australia) and cultured in Media 200 (Invitrogen) supplemented with LSGS Low Serum Growth Supplement (Invitrogen) unless otherwise stated.

All animal procedures reported below were carried out with animal ethics approval from the institution where the work was performed. Experiments using the DMH colon cancer model were run under *NHMRC Australian code of practice for the care and use of animals for scientific purposes* (7th Edition 2004), whilst studies using the DLD-1 colon adenocarcinoma model were conducted following UKCCCR guidelines (Workman *et al*, 1998) under a project licence issued by the UK Home Office.

Cell culture

HUVEC were cultivated in M199 basic medium with HEPES buffer (Invitrogen #12340), with 20% Fetal Bovine Serum (FBS) supplemented with L-glutamine and 100U/ml penicillin/streptomycin and ECGF at 200ng/ml (endothelial cell growth factor, Roche # 11 033 484 001) on gelatin coated plates.

HUVEC morphology

HUVEC cells were seeded at two different densities onto 24 well tissue culture plate (20000 cells/well), were cultured for 4 d and monitored until the cells reached confluency. Representative fields of view for both cell densities were selected for photographic recording. Both confluent and non-confluent cells were photographed under three different magnifications (10X and 40X). Cells were then treated with two concentrations of CYT997 (10 nM and 100 nM) for 1 h. The changes in treated cells were monitored under a microscope and photographed in the same manner as untreated cells.

HUVEC Proliferation Assay

JPET Fast Forward. Published on September 14, 2011 as DOI: 10.1124/jpet.111.186965
This article has not been copyedited and formatted. The final version may differ from this version.

Cells ($1x10^4$) were plated in flat-bottomed 96 well plates and were allowed to adhere overnight in M199 medium + 1% FBS. Compounds were added at the concentrations indicated, in fresh medium containing 0.1% DMSO. After 1 h incubation at 37 °C, VEGF (Recombinant Human VEGF121 , R&D Systems #298-VS) was added (10 ng/mL final concentration). After 5 d at 37 °C, 5% CO_2, Alamar Blue (10 μL) was added for the final 4-6 h of the culture and fluorescence then read at an excitation wavelength of 544 nM and an emission wavelength of 590 nM with a Polarstar plate reader (BMG LABTECH, Germany).

In Vivo Tumor Models

Metastatic Colon Cancer Model. The colon cancer liver metastases model was used as previously described (Malcontenti-Wilson *et al* 2001). Male CBA mice (Laboratory Animal Services, Adelaide, Australia) were inoculated intrasplenically with 5×10^4 mouse DMH colon cancer cells followed by splenectomy. Mice were allocated at random to treatment groups on Day 9. CYT997 tartrate salt in 0.1 M Captisol (equivalent to 5, 10, or 15 mg free base /kg/day; n = 14 mice/group) or 0.1 M Captisol (10 mL/kg, n = 12 mice) and were dosed i.p. twice daily, 12 h apart. Mice were killed after 11 d of treatment and wet liver weight measured. A dose of 15mg/kg/day was tolerated by mice, however 2 mice were assessed as requiring euthanasia prior to endpoint (2/14 or 14%). The percentage of liver volume occupied by metastases was calculated using quantitative stereological assessment as described below.

Determination of metastatic burden. Mice were weighed at the endpoint and livers and other organs placed in formalin. After 2 d, livers were placed in a solution of 50% ethanol and after removing excess fluid, the wet weights of all livers were determined. Stereological assessment of liver metastases was performed as follows.

Each liver (after being fixed in formalin for 4 d) was cut into 1.5-mm slices using a multi-blade fractionator, and alternate slices used for measurement. Images of the slices were captured using digital imaging and an Image Analysis software program (Image Pro Plus, Media Cybernetics, Perth, Australia) was used to determine tumor load using stereological principles.

Microvascular Corrosion Casting: Following the procedure described previously (Malcontenti-Wilson *et al*, 2001) the thorax of tumor bearing animals from the DMH colon cancer model described above, was opened to expose the heart and thoracic vessels. The aorta was cannulated with a 24 gauge catheter and the vasculature was flushed with warm saline solution containing heparin (10 IU/mL), papaverine (12 mg/mL) and 6% polyvinyl pyrrolidinone (PVP40) (Sigma, Australia). The effluent was discharged through a right atrial puncture, and once clear, followed by the infusion of an acrylic resin of Mercox CL-2B (Okenshoji Co, Tokyo, Japan), methyl methacrylate (Sigma) and catalyst MA (Vilene Med Co., Japan) infused at a pressure of 160 mmHg to allow microvascular filling. After polymerization of the resin overnight, the liver was excised and tissue was digested in 20% potassium hydroxide at 37 °C for a minimum of 2 d. Once the digestion process was complete the resulting resin casts were then frozen and cut into sections with a high speed cutting tool. The casts were washed in distilled water, dried at 37 °C and mounted on aluminium stubs with electrodag 415 (Acheson Colloids, Michigan, USA). Specimens were gold coated with a Baltec SCD005 sputtercoater and viewed on a scanning electron microscope (Hitachi 570 SEM). Scanning electron micrograph digital images from each specimen were captured at various magnifications using Spectrum Imaging software. Several tumors and normal liver were examined from every animal in each group.

Colon adenocarcinoma model: Female Balb/C immunodeficient nude mice aged 6-12 weeks (Harlan, Loughborough, UK) were used. Tumors were excised from a donor animal, placed in sterile physiological saline containing penicillin and streptomycin and cut into small fragments of approximately 2mm. Under brief general isoflurane inhalation anaesthesia, DLD-1 fragments were implanted in both the left and right flanks of each mouse. Once tumors had reached a volume of approximately 150 mm^3 (as measured by callipers), indicating that an established tumor vascular network was present, the mice were allocated into groups of three by restricted randomisation to keep group mean tumor size variation to a minimum.

Determination of Vascular Shutdown: Mice were treated with a single dose of CYT997 (40 mg/kg, as dihydrochloride) by oral gavage (three groups) and a vehicle (saline) treated group was maintained as a control. At 1, 6 or 24 h following CYT997 treatment, vascular shutdown was assessed as follows: Hoechst 33342 dye was dissolved in sterile saline and injected intravenously by the tail vein at 40 mg/kg. One min after injection the mice in the relevant treatment group were sacrificed by cervical dislocation and the tumors carefully and rapidly excised. One tumor from each mouse was then wrapped in aluminium foil, immediately immersed in liquid nitrogen and stored at -80 °C until ready for ultracryotomy. The other tumor was immersion fixed in 10% neutral buffered formalin for 24 h and processed for paraffin embedding. The control group were processed at the same time as the 24 h cohort.

Frozen sections of 10 μm thickness were taken at approximately 100 μm intervals through the tumor. Up to five fields from each of 10 random sections were examined for each tumor under UV illumination using a Leica DMRB microscope, with images captured digitally through a JVC 3-CCD camera and processed using AcQuis (Synoptics, Cambridge, UK) software. Functional vasculature was assessed by

placing a cm^2 grid over the captured digital image and counting the number of points on the grid overlaying fluorescently stained cells. The percentage functional vasculature was calculated by taking the total number of fluorescence-positive points for each field and dividing by the total number of points. An average percentage for each animal was calculated. Comparisons were made between percentage vasculature in control and treated tumors. Statistical analysis of shutdown was carried out using a one way ANOVA with a post hoc pairwise comparison.

Dose effect on Vascular Shutdown: Tumor-bearing mice obtained as described above (n=3 per group) were treated with a single oral dose of either 10, 20 or 40 mg/kg CYT997 or vehicle control by oral gavage. At 1 h following treatment, vascular shutdown was assessed as described above.

Results

CYT997 affects HUVEC morphology in vitro. To elucidate activity of CYT997 upon tumor endothelium, the effects of the compound on HUVEC cells in culture were studied. The morphological changes wrought upon the HUVEC monolayer by CYT997 were visualised using microscopy and are depicted in Figure 1. There is minimal effect on cells exposed to 10 nM CYT997 after 1h; however, there is a profound alteration in cell shape and clear disruption of monolayer confluency for cells exposed to 100 nM CYT997. At this dose and time, the cells are clearly rounded up with significant membrane blebbing apparent.

CYT997 is cytotoxic to proliferating HUVEC cells in vitro. To determine the effect of longer term exposure of CYT997 to HUVEC cells, increasing concentrations of CYT997 and a selection of other tubulin binding agents were added to VEGF-

stimulated HUVECs grown in culture, and proliferation determined by Alamar Blue assay after 72 h. As shown in Figure 2, CYT997 inhibited the proliferation of HUVEC cells with an IC_{50} of 3.7 ± 1.8 nM (SD), and at doses above 10 nM diminished cell viability. Similar data was obtained for CA4P and vinblastine (IC_{50}s 3.1 ± 2.7 nM and 0.9 ± 1.0 nM respectively) in agreement with published results (Vincent *et al*, 2005; Vacca *et al*, 1999). Doxorubicin also caused complete destruction of viable cells though at much higher concentrations (IC_{50} >2 μM). In contrast, at the concentrations tested, paclitaxel inhibited VEGF stimulated growth, but did not cause loss of viable cells, demonstrating a cytostatic rather than cytotoxic effect, as reported previously (Pasquier *et al*, 2004).

CYT997 is active in the DMH metastatic Colon Cancer Model and disrupts the vasculature of hepatic metastases. The dimethyl hydrazine (DMH) metastatic colon cancer liver metastasis model is a well validated model that has been used to study the anti-metastatic effects and vascular disrupting properties of CA4P and other VDAs (Malcontenti-Wilson *et al*, 2001, 2008; Chan *et al*, 2007). CYT997 was therefore profiled in this model with CA4P as positive control.

Quantitative stereological assessment of the number and volume of metastatic nodules in livers of tumor bearing mice were determined after 11 days of treatment with CYT997 (i.p., b.i.d.) Doses of both 10 and 15 mg/kg/day of CYT997 significantly reduced the total wet weight of the liver compared to control (Figure 3A). The percentage of liver volume occupied by metastases was also dramatically reduced in a dose-dependent manner (Figure 3B). In addition, macroscopic examination of the liver clearly showed a dose-dependent reduction in tumor burden with some livers being essentially tumor-free in the 10 and 15 mg/kg cohorts (Supplemental Figure 1).

The effect of CYT997 on tumor endothelium *in vivo* was determined by corrosion casting of tumor microvasculature in the metastatic lesions and imaged using scanning electron microscopy. Figure 4A depicts typical images from untreated liver metastases, where a dense, tortuous microvascular network is observed and heterogeneous vasculature with variations in tumor vessels diameter is also evident. A single dose of CYT997 (7.5 mg/kg, <30% of the MTD) was shown to cause extensive disruption to the tumor vasculature *in vivo* (Figure 4B). Tumors demonstrated large areas with absence of vessels, indicating vessel occlusion or damage (Figures 4B, panels A and C). An obvious reduction in the density of patent vessels was seen. Extravasation of resin is apparent in some areas where damaged vessels may allow escape of casting material through gaps in the endothelial wall (Figures 4B, panels B and D). Normal liver vasculature, however, appeared unaffected by treatment with CYT997. The data obtained for CYT997 shows similarities to that obtained for CA4P dosed at 100 mg/kg which was investigated concurrently as a positive control (data not shown), and with data reported previously (Malcontenti-Wilson *et al*, 2001).

Single dose CYT997 causes time and dose-dependent vascular shutdown. Having established that CYT997 causes profound disruption to tumor vasculature, a separate study of the dose-response and pharmacodynamics of this effect with oral administration was undertaken. Athymic nude mice bearing subcutaneous DLD-1 human colon adenocarcinoma xenografts (~150 mm^3 in size) were dosed with CYT997 (40 mg/kg, p.o. ~80% of MTD), and at 1, 6 or 24 h post-CYT997 treatment vascular shutdown was assessed by injection of Hoechst 33342 dye (40 mg/kg) and determination of dye fluorescence in tumor cross-sections (Figure 5 A and B). Vascular shutdown was evident over the study period (approximately 93%, 77% and

70% shutdown respectively; $p<0.01$) with a non-statistical trend to apparent recovery observed at 6 and 24 h. Histological evaluation of haematoxylin and eosin stained sections showed a notable increase in the amount of necrosis in the DLD-1 tumors at 24 h post CYT997 (data not shown). The delay in the appearance of necrosis presumably reflects the delay in tumor cell response post-treatment, following loss of blood supply.

In a separate experiment, the dose-dependency of vascular shutdown was determined. Animals received a single oral dose of 10, 20 or 40 mg/kg CYT997 (or vehicle control) 1 h prior to assessment of vascular shutdown, which was performed as described above. Doses of 40 mg/kg and 20 mg/kg resulted in shutdown of approximately 98.6% and 94.4% respectively, both of which were highly significant relative to the untreated control tumors ($p<0.001$; Figure 5C). The lowest dose tested, 10 mg/kg, lead to a less profound but still significant effect ($p=0.03$), with approximately 60.6% shutdown in tumor vasculature observed 1 h post dose.

Discussion

The development of anticancer drugs with an improved therapeutic window through the selective targeting of drugs to cancerous tissue has become a major focus in oncology drug development. Compounds that selectively impact the vasculature of tumors have been the focus of considerable attention in recent years, and anti-angiogenesis agents that inhibit tumor neovascularization, such as bevacizumab, sunitinib and sorafenib, are now marketed for the treatment of certain vascularised solid tumors (Markland *et al* 2010). Vascular disrupting agents are a related but separate class of compounds that disrupt the existing vasculature in tumors and promising data has been reported from clinical trials of the more advanced compounds in this class (Anderson *et al*, 2003; Hande *et al*, 2001).

CYT997 is a structurally novel, orally active VDA discovered in our laboratories (Burns *et* al 2009a), which has successfully completed two Phase I clinical trials (Lickliter *et al*, 2010; Francesconi *et al*, 2009). Preliminary anti-vascular activity of the compound has been reported (Burns *et* al 2009b) and in this paper we have described further studies to better understand the vascular disrupting effects of the compound with particular regard to dose and functional activity in *in vivo* tumor models.

Thus, the well characterised DMH colon cancer liver metastases model was used to assess the anti-metastatic and VDA activity of CYT997. In this model metastatic lesions develop in the liver of CBA mice 21 days after inoculation of cells from a DMH induced primary colon cancer cell line maintained in donor mice. Mice treated with CYT997 (i.p., b.i.d.) for 11 days from day 9 after tumor cell inoculation showed a dose-dependent reduction in liver weight, which was used as a surrogate measure of tumor burden, compared to vehicle control (Figure 3A). The percentage of liver volume occupied by metastases was also dramatically reduced in a dose-dependent manner (Figure 3B). In addition, macroscopic examination of the liver clearly showed a dose-dependent reduction in tumor burden with some livers being essentially tumor-free in the 10 and 15 mg/kg/day cohorts (Supplementary material).

In a separate study using this model, CYT997 showed a dramatic impact on the distribution and penetration of a polymer into the vascular bed of the liver metastases in corrosion cast experiments. Thus, a single dose of CYT997 resulted in dramatic reductions in the density of tumor blood vessels both centrally and at the tumor-liver margin in the vasculature of hepatic metastases. The tumor microvasculature of these metastases in control animals are shown to be continuous with normal liver sinusoids. In contrast, CYT997 treated tumor-bearing livers demonstrated loss of continuity with

the liver sinusoids, most likely as a result of the lack of resin penetration at sites of blocked vasculature. Significant extravasation of the resin was also apparent, manifesting as plaques of resin material at the margin of the metastasis. Importantly, the profound differences in the intra-tumoral microvasculature of CYT997-treated tumors were not accompanied by significant changes in the microvasculature of the surrounding normal liver, as the fine, evenly distributed liver sinusoidal pattern can clearly be seen adjacent to the areas of disrupted tumor vasculature.

The catastrophic effect CYT997 has on tumor microvasculature was also measured using the fluorescent dye Hoecsht 33342 in a xenograft model using the human DLD-1 colon adenocarcinoma cell line. In this model a single oral dose of CYT997 (40 mg/kg) reduced functional vasculature in tumors with a maximal effect at 1 h post CYT997 dose, and with minimal recovery over 24 h. The disruption to tumor blood flow at 1 h after CYT997 dosing was shown to be dose-dependent with a dose of 10 mg/kg (~20% of MTD) showing ~60% reduction in tumor blood flow compared with control treated animals. In these studies it is apparent that tumor cells at the periphery of the tumor are resistant to the anti-vascular effects of drug, an effect that has also been observed with other VDAs (Dark *et al* 1997; Chan *et al* 2008). These peripheral cells define the viable rim of the tumor and are recognised as a resistance mechanism to VDAs in cancer treatment, possibly leading to tumor revascularisation and regrowth (*vide infra*). Preclinical studies have shown that combinations of VDAs and cytotoxic agents or angiogenesis inhibitors can overcome this resistance in certain instances (Shi and Siemann, 2005; Horsman and Siemann 2006) which has led to clinical studies of VDAs in combination with either cytotoxic or anti-angiogenesis agents.

The detailed mechanisms by which VDAs cause such profound vascular damage in tumors are not fully understood and are the subject of ongoing research in a number of laboratories. Most VDAs inhibit microtubule polymerisation and it appears that the immature endothelial cells of tumor microvasculature are more susceptible to the effects of tubulin-binding agents as these cells are more reliant on the microtubule network for cellular integrity (Davis *et al*, 2002). The precise biochemical processes occurring within endothelial cells leading to the reported effects, however, have not been fully elucidated (Kanthou and Tozer, 2009). Activation of Rho kinase and MAP kinase signalling pathways have been observed in endothelial cells treated with VDAs as have effects on VE-cadherin (Kanthou and Tozer 2002; Vincent *et al*, 2005). Indeed, the Rho-kinase inhibitor Y-27632 has been shown to antagonise the vascular disruption caused by CA4P in an *in vivo* xenograft model (Kanthou and Tozer 2002), whilst neutralizing mAbs to VE-cadherin have been shown to synergise with CA4P in vivo (Vincent *et al*, 2005).

Morphological changes to endothelial cells after treatment with VDAs, including membrane blebbing, have been observed in both *in vitro* and *in vivo* studies (Kanthou and Tozer, 2002; Yeung *et al*, 2007; Bonezzi *et al*, 2009), and the rounding-up and blebbing clearly apparent in HUVEC cells exposed to CYT997 (Figure 1) is thus fully consistent with this literature data. Clearly such morphological changes would be expected to have a significant impact on tumor microvessel integrity leading to an increase in tumor vascular permeability, as has been reported for other VDAs (Tozer *et* al 2005b; Reyes-Aldasoro *et* al 2008).

Whilst the ablative effects on tumor vasculature for tumors treated with CYT997 and other VDAs are significant, it is clear from preclinical studies with other VDAs that tumor microvasculature is rapidly re-established on cessation of drug dosing. The

process appears to arise from a drug-induced spike in bone marrow–derived circulating endothelial progenitor cells (CEPs) that locate to the viable rim remaining after VDA treatment (Shaked *et al* 2006; Ferace *et al* 2007), most likely driven by cytokines such as G-CSF, VEGF and SDF-1, levels of which are elevated after VDA treatment (Shaked *et al*, 2009). Whilst most VDAs studied to date are given intravenously, thereby limiting dosing frequency in the clinical setting, the oral activity of CYT997 allows for frequent (e.g. daily) dosing which would presumably lead to repeated vascular insult, even at the sub-MTD doses demonstrated herein. Whether such a dosing regimen is more effective in targeting the revascularization and tumor regrowth processes discussed above remains to be determined and will be the subject of further studies.

The collected data for CYT997 reported in this paper and our earlier disclosure (Burns *et* al, 2009b) clearly demonstrate that the compound has significant effects on endothelial cells grown in culture, and profound vascular disrupting activity *in vivo*. The effects parallel those reported for CA4P and other VDAs, and it is likely that the biochemical mechanisms underlying the anti-vascular effects are similar. In the clinic, the oral bioavailability of CYT997, allowing for more frequent administration, may prove beneficial in minimising the tumor revascularisation observed with other intravenously dosed VDAs. Taken together we believe these studies reported herein support the ongoing development of this promising new VDA.

Acknowledgements

Dr Robert Kapsa and Dr Anita Quigley (Department of Clinical Neurosciences, St. Vincent's Hospital, Fitzroy, Australia) are thanked for assistance in obtaining the microscopy images, Figure 1.

Authorship contributions

Participated in research design: Burns, Fantino, Wilks, Phillips, Powell, Shnyder, Smith

Conducted experiments: Segal, Joffe, Cooper, Nelson, Dubljevic, Malcontenti-Wilson

Contributed new reagents or analytic tools: Harte, Christophi

Performed data analysis: Burns, Fantino, Wilks, Phillips, Powell, Shnyder, Malcontenti-Wilson

Wrote or contributed to the writing of the manuscript: Burns, Segal, Shnyder, Smith, Wilks, Malcontenti-Wilson

References

Anderson HL, Yap JT, Miller MP, Robbins A, Jones T and Price PM (2003) Assessment of pharmacodynamic vascular response in a phase I trial of combretastatin A4 phosphate. *J Clin Oncol* **21**:2823-2830.

Bayless KJ and Davis GE (2004) Microtubule depolymerization rapidly collapses capillary tube networks in vitro and angiogenic vessels in vivo through the small GTPase Rho. *J Biol Chem* **279**:11686-11695.

Bonezzi K, Taraboletti G, Borsotti P, Bellina F, Rossi R and Giavazzi R (2009) Vascular disrupting activity of tubulin-binding 1,5-diaryl-1H-imidazoles. *J Med Chem* **52**:7906-7910.

Burns CJ, Harte MF, Bu X, Fantino E, Joffe M, Sikanyika H, Su S, Tranberg CE, Wilson N, Charman SA, Shackleford DM and Wilks AF (2009a) Discovery of CYT997: a structurally novel orally active microtubule targeting agent. *Bioorg Med Chem Lett* **19**:4639-4642.

Burns CJ, Fantino E, Phillips ID, Su S, Harte MF, Bukczynska PE, Frazzetto M, Joffe M, Kruszelnicki I, Wang B, Wang Y, Wilson N, Dilley RJ, Wan SS, Charman SA, Shackleford DM, Fida R, Malcontenti-Wilson C and Wilks AF (2009b) CYT997: a novel orally active tubulin polymerization inhibitor with potent cytotoxic and vascular disrupting activity in vitro and in vivo. *Mol Cancer Ther* **8**:3036-3045.

Chan LS, Malcontenti-Wilson C, Muralidharan V and Christophi C (2007) Effect of vascular targeting agent Oxi4503 on tumor cell kinetics in a mouse model of colorectal liver metastasis. *Anticancer Res* **27**:2317-2323.

Chan LS, Malcontenti-Wilson C, Muralidharan V and Christophi C (2008) Alterations in vascular architecture and permeability following OXi4503 treatment. *Anticancer Drugs* **19**:17-22.

Davis PD, Dougherty GJ, Blakey DC, Galbraith SM, Tozer GM, Holder AL, Naylor MA, Nolan J, Stratford MRL, Chaplin DJ and Hill SA (2002) ZD6126: a novel vascular-targeting agent that causes selective destruction of tumor vasculature. *Cancer Res* **62**: 7247–7253.

Dark GG, Hill SA, Prise VE, Tozer GM, Pettit GR and Chaplin DJ (1997) Combretastatin A-4, an agent that displays potent and selective toxicity toward tumor vasculature. *Cancer Res* **57**:1829-1834.

El-Emir E, Boxer GM, Petrie IA, Boden RW, Dearling JL, Begent RH and Pedley RB (2005) Tumor parameters affected by combretastatin A-4 phosphate therapy in a human colorectal xenograft model in nude mice. *Eur J Cancer* **41**:799-806.

Farace F, Massard C, Borghi E, Bidart JM and Soria JC (2007) Vascular disrupting therapy-induced mobilization of circulating endothelial progenitor cells. *Ann Oncol* **18**:1421-1422.

Francesconi, A, Kotasek, D, Burge M, Smith G, Lickliter J (2009) Phase I evaluation of orally-administered CYT997, a novel cytotoxic vascular-disrupting agent, in patients with advanced cancer. *J Clin Oncol* **27**:15s (suppl; abstr 3568)

Hamel E (1996) Antimitotic natural products and their interactions with tubulin. *Med Res Rev* **16**:207-231.

Hande KR, Hagey A, Berlin J, Cai Y, Meek K, Kobayashi H, Lockhart AC, Medina D, Sosman J, Gordon GB and Rothenberg ML (2006) The pharmacokinetics

and safety of ABT-751, a novel, orally bioavailable sulfonamide antimitotic agent: results of a phase 1 study. *Clin Cancer Res* **12**:2834-2840.

Hearn BR, Shaw SJ, Myles DC (2007) Microtubule Targeting Agents. In *Comprehensive Medicinal Chemistry II* (Taylor JB and Triggle DJ eds) pp 81-110, Elsevier, Amsterdam.

Honore S, Pasquier E and Braguer D (2005) Understanding microtubule dynamics for improved cancer therapy. *Cell Mol Life Sci* **62**:3039-3056.

Hori K and Saito S (2004) Induction of tumor blood flow stasis and necrosis: a new function for epinephrine similar to that of combretastatin A-4 derivative AVE8062 (AC7700). *Br J Cancer* **90**:549-553.

Horsman MR and Siemann DW (2006) Pathophysiologic effects of vascular-targeting agents and the implications for combination with conventional therapies. *Cancer Res* **66**:11520-11539.

Kanthou C and Tozer GM (2002) The tumor vascular targeting agent combretastatin A-4-phosphate induces reorganization of the actin cytoskeleton and early membrane blebbing in human endothelial cells. *Blood* **99**:2060-2069.

Kanthou C and Tozer GM (2009) Microtubule depolymerizing vascular disrupting agents: novel therapeutic agents for oncology and other pathologies. *Int J Exp Pathol* **90**:284-294.

Lickliter JD, Francesconi AB, Smith G, Burge M, Coulthard A, Rose S, Griffin M, Milne R, McCarron J, Yeadon T, Wilks A, Cubitt A, Wyld DK and Vasey PA (2010) Phase I trial of CYT997, a novel cytotoxic and vascular-disrupting agent. *Br J Cancer* **103**:597-606.

Luo Y, Hradil VP, Frost DJ, Rosenberg SH, Gordon GB, Morgan SJ, Gagne GD, Cox BF, Tahir SK and Fox GB (2009) ABT-751, a novel tubulin-binding agent, decreases tumor perfusion and disrupts tumor vasculature. Anticancer Drugs 20:483-492.

Malcontenti-Wilson C, Chan L, Nikfarjam M, Muralidharan V and Christophi C (2008) Vascular targeting agent Oxi4503 inhibits tumor growth in a colorectal liver metastases model. *J Gastroenterol Hepatol* **23**:e96-e104.

Malcontenti-Wilson C, Muralidharan V, Skinner S, Christophi C, Sherris D and O'Brien PE (2001) Combretastatin A4 prodrug study of effect on the growth and the microvasculature of colorectal liver metastases in a murine model. *Clin Cancer Res* **7**:1052-1060.

Markland FS, Swenson S, Minea R (2010) *Tumor Angiogenesis: From Molecular Mechanisms to Targeted Therapy*. Wiley-VCH, Hoboken.

Nicholson B, Lloyd GK, Miller BR, Palladino MA, Kiso Y, Hayashi Y and Neuteboom ST (2006) NPI-2358 is a tubulin-depolymerizing agent: in-vitro evidence for activity as a tumor vascular-disrupting agent. *Anticancer Drugs* **17**:25-31.

Pasquier E, Carre M, Pourroy B, Camoin L, Rebai O, Briand C and Braguer D (2004) Antiangiogenic activity of paclitaxel is associated with its cytostatic effect, mediated by the initiation but not completion of a mitochondrial apoptotic signaling pathway. *Mol Cancer Ther* **3**:1301-1310.

Pettit GR, Temple C, Jr., Narayanan VL, Varma R, Simpson MJ, Boyd MR, Rener GA and Bansal N (1995) Antineoplastic agents 322. synthesis of combretastatin A-4 prodrugs. *Anticancer Drug Des* **10**:299-309.

Reyes-Aldasoro CC, Wilson I, Prise VE, Barber PR, Ameer-Beg M, Vojnovic B, Cunningham VJ and Tozer GM (2008) Estimation of apparent tumor vascular permeability from multiphoton fluorescence microscopic images of P22 rat sarcomas in vivo. *Microcirculation* **15**:65-79.

Schwartz EL (2009) Antivascular actions of microtubule-binding drugs. *Clin Cancer Res* **15**:2594-2601.

Shaked Y, Ciarrocchi A, Franco M, Lee CR, Man S, Cheung AM, Hicklin DJ, Chaplin D, Foster FS, Benezra R and Kerbel RS (2006) Therapy-induced acute recruitment of circulating endothelial progenitor cells to tumors. *Science* **313**:1785-1787.

Shaked Y, Tang T, Woloszynek J, Daenen LG, Man S, Xu P, Cai SR, Arbeit JM, Voest EE, Chaplin DJ, Smythe J, Harris A, Nathan P, Judson I, Rustin G, Bertolini F, Link DC and Kerbel RS (2009) Contribution of granulocyte colony-stimulating factor to the acute mobilization of endothelial precursor cells by vascular disrupting agents. *Cancer Res* **69**:7524-7528.

Shi W and Siemann DW (2005) Targeting the tumor vasculature: enhancing antitumor efficacy through combination treatment with ZD6126 and ZD6474. *In Vivo* **19**:1045-1050.

Tozer GM, Ameer-Beg SM, Baker J, Barber PR, Hill SA, Hodgkiss RJ, Locke R, Prise VE, Wilson I and Vojnovic B (2005a) Intravital imaging of tumor vascular networks using multi-photon fluorescence microscopy. *Adv Drug Deliv Rev* **57**:135-152.

Tozer GM, Kanthou C and Baguley BC (2005b) Disrupting tumor blood vessels. *Nat Rev Cancer* **5**:423-435.

Vacca A, Iurlaro M, Ribatti D, Minischetti M, Nico B, Ria R, Pellegrino A and Dammacco F (1999) Antiangiogenesis is produced by nontoxic doses of vinblastine. *Blood* **94**:4143-4155.

van Ark-Otte J, Samelis G, Rubio G, Lopez Saez JB, Pinedo HM and Giaccone G (1998) Effects of tubulin-inhibiting agents in human lung and breast cancer cell lines with different multidrug resistance phenotypes. *Oncol Rep* **5**:249-255.

Vincent L, Kermani P, Young LM, Cheng J, Zhang F, Shido K, Lam G, Bompais-Vincent H, Zhu Z, Hicklin DJ, Bohlen P, Chaplin DJ, May C and Rafii S (2005) Combretastatin A4 phosphate induces rapid regression of tumor neovessels and growth through interference with vascular endothelial-cadherin signaling. *J Clin Invest* **115**:2992-3006.

Yeung SC, She M, Yang H, Pan J, Sun L and Chaplin D (2007) Combination chemotherapy including combretastatin A4 phosphate and paclitaxel is effective against anaplastic thyroid cancer in a nude mouse xenograft model. *J Clin Endocrinol Metab* **92**:2902-2909.

Yin S, Cabral F and Veeraraghavan S (2007) Amino acid substitutions at proline 220 of beta-tubulin confer resistance to paclitaxel and colcemid. *Mol Cancer Ther* **6**:2798-2806.

Footnotes

This work was supported by an AusIndustry START Grant, and additional funding by Cytopia Research Pty Ltd (now YM BioSciences Australia).

This work has previously been presented in part in Poster form at 2005 AACR Conference (San Diego, USA) and 22nd Lorne Cancer Meeting 2010 (Lorne, Australia).

Legends for Figures

Figure 1

CYT997 disrupts endothelial cells monolayers and causes morphological changes. HUVEC grown in monolayers were treated with 10 or 100 nM of CYT997 for one hour and the cell morphology was visualized by light microscopy at 10X (A) or 40X (B) magnification. (A) CYT997 (100 nM) caused disruption of the endothelial monolayer compared to cells treated with CYT997 (10 nM); (B) Most cells treated with CYT997 (100 nM) adopted a retracted, rounded morphology with a granular surface, compared to a typical spread out endothelial cell in the same field.

Figure 2

CYT997 inhibits proliferation of endothelial cells. HUVEC were stimulated with VEGF and treated with compounds as indicated. Viability was measured after 5 days using the metabolic indicator Alamar Blue. The fluorescence levels of control samples containing no cells (medium), unstimulated cells (-VEGF) and stimulated cells (+VEGF) are indicated. The experiment was repeated 3 times with similar results. A representative experiment is shown.

Figure 3

Assessment of tumor burden. Percentage of liver metastases was significantly reduced with all three doses of CYT997 in a dose dependent manner. A. Tumor weight was significantly reduced, dose dependently, with 5mg/kg/day, 10mg/kg/day and 15mg/kg/day of CYT997 (i.p., b.i.d.) when administered from day 11-21 after tumor induction (mean ± SD). Statistical analysis performed using Student's t-Test, two-samples assuming unequal variances. Liver weights in normal mice (no tumor) was 1.18 ± 0.09 g (n=7). B. Percentage of liver metastases was significantly reduced with

all three doses of CYT997 in a dose dependent manner (mean ± SD). Statistical analysis performed using Student's t-Test, two-samples assuming unequal variances.

Figure 4

CYT997 disrupts tumor microvascular architecture in a mouse model of colorectal liver metastases. Scanning electron micrographs of microvascular resin casts of liver metastases. A. Representative micrographs of typical microvascular architecture of untreated tumors showing dense tortuous tumor microvasculature, flattened dilated vessels and connections of tumor vessels with normal liver sinusoids; B Representative micrographs of liver metastases 6 h after treatment with a single dose of CYT997 (7.5mg/kg, i.p.), depicting disruption of tumor blood vessels. Areas of incomplete filling, spindly branches of vessels tapering towards area of occlusion, and masses of extravasated resin are seen. Some vessels remaining at the tumor margin are dilated and flattened, then end abruptly.

Figure 5

CYT997 reduces functional vasculature in xenograft tumor model. A. Time-dependant vascular shutdown of DLD-1 human colon adenocarcinoma xenografts following a single oral dose of CYT997 at 40 mg/kg relative to vehicle (mean ± SD); B. Representative images of DLD-1 human colon adenocarcinoma xenografts showing functional vasculature using Hoechst 33342 staining, following a single oral dose of CYT997 (40 mg/kg) at 1, 6 and 24h post dose; C. Dose dependent vascular shutdown of DLD-1 human colon adenocarcinoma xenografts assessed 1 h after a single oral dose of CYT997 at 10, 20 or 40 mg/kg relative to vehicle (mean ± SD)

JPET Fast Forward. Published on September 14, 2011 as DOI: 10.1124/jpet.111.186965
This article has not been copyedited and formatted. The final version may differ from this version.

Figure 1

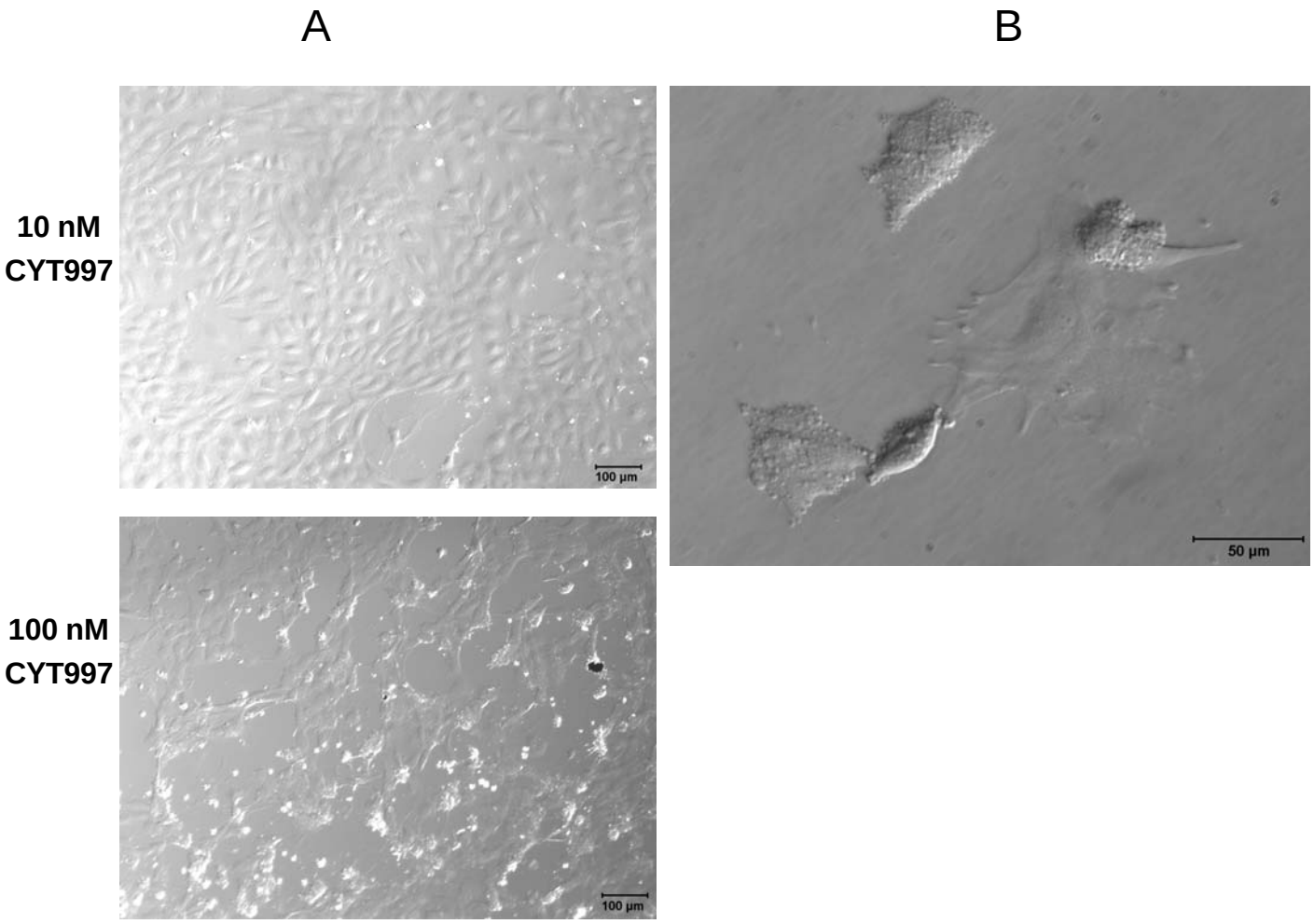

JPET Fast Forward. Published on September 14, 2011 as DOI: 10.1124/jpet.111.186965
This article has not been copyedited and formatted. The final version may differ from this version.

Figure 2

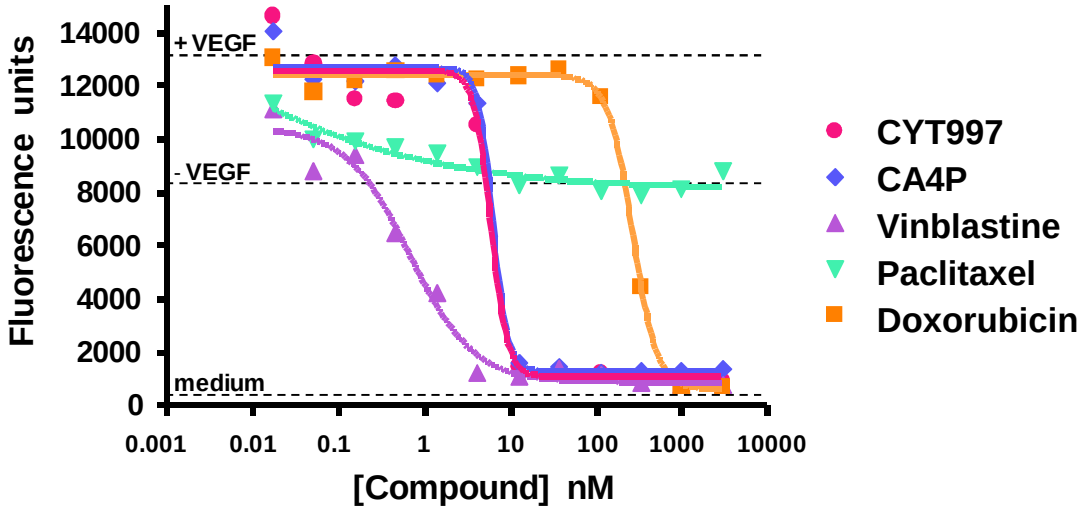

JPET Fast Forward. Published on September 14, 2011 as DOI: 10.1124/jpet.111.186965
This article has not been copyedited and formatted. The final version may differ from this version.

Figure 3

A

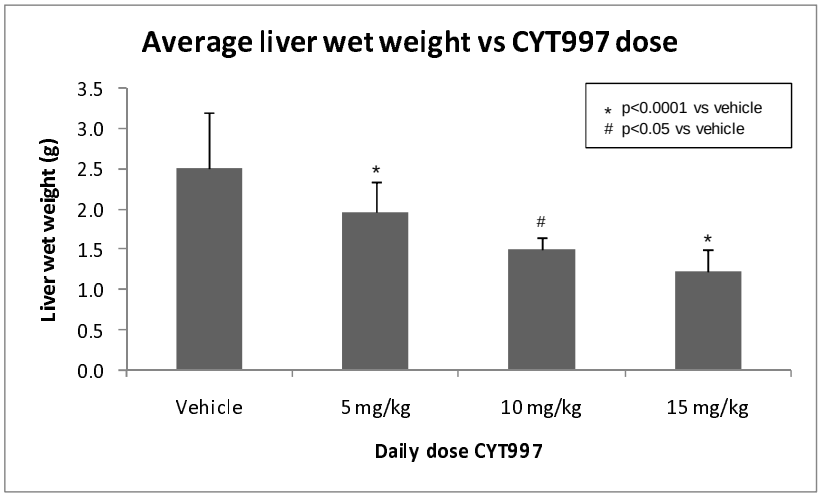

B

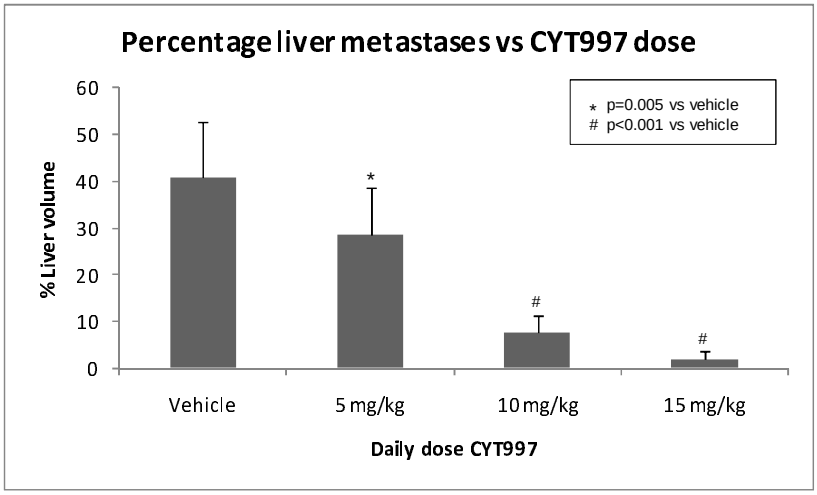

JPET Fast Forward. Published on September 14, 2011 as DOI: 10.1124/jpet.111.186965
This article has not been copyedited and formatted. The final version may differ from this version.

Figure 4

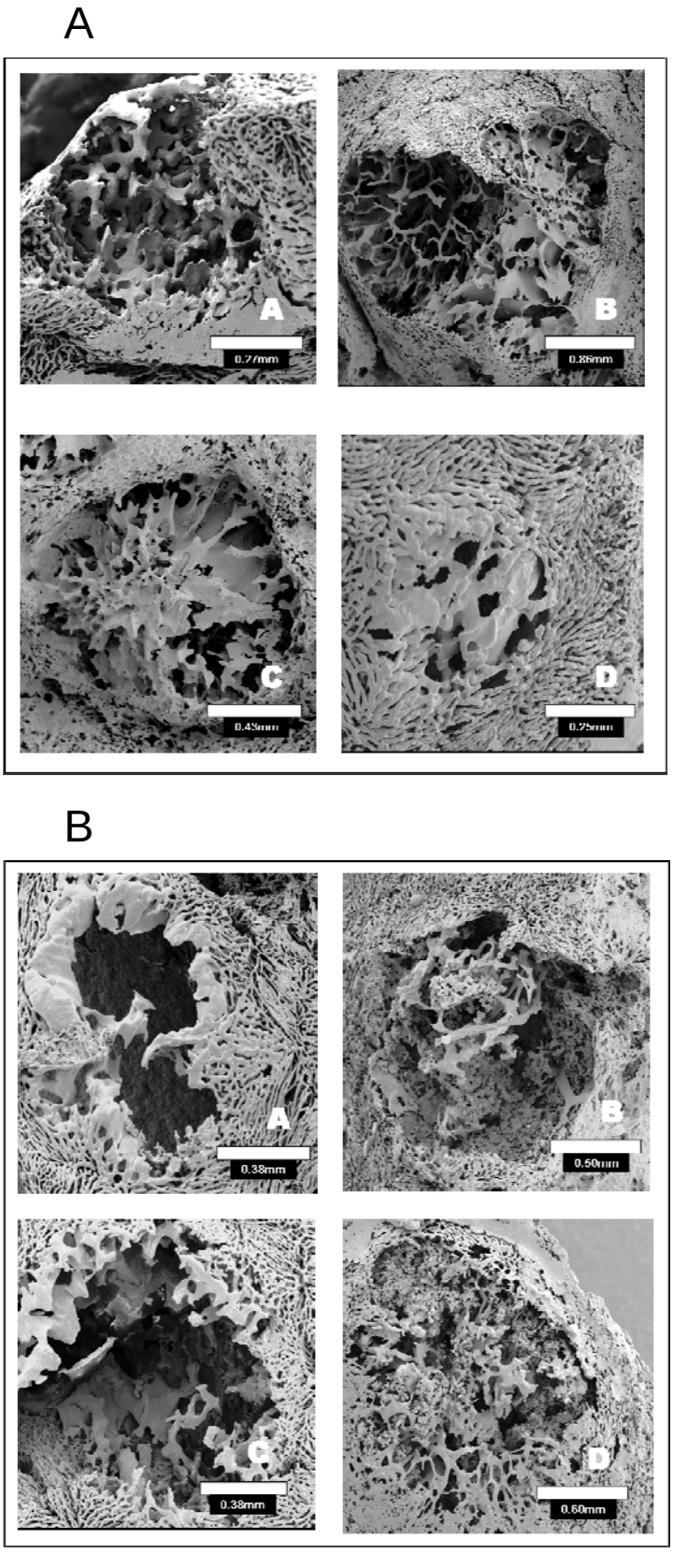

JPET Fast Forward. Published on September 14, 2011 as DOI: 10.1124/jpet.111.186965
This article has not been copyedited and formatted. The final version may differ from this version.

Figure 5

A

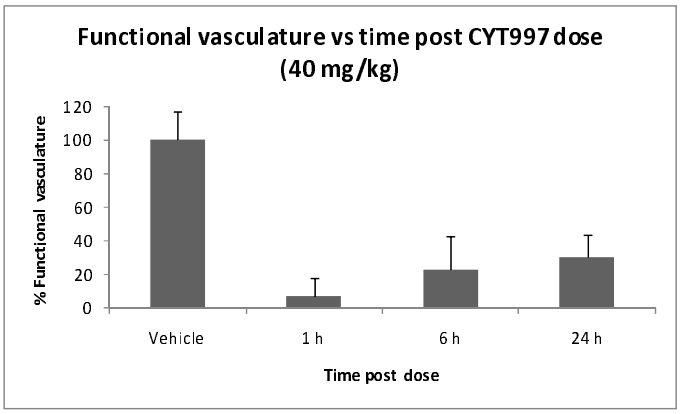

B

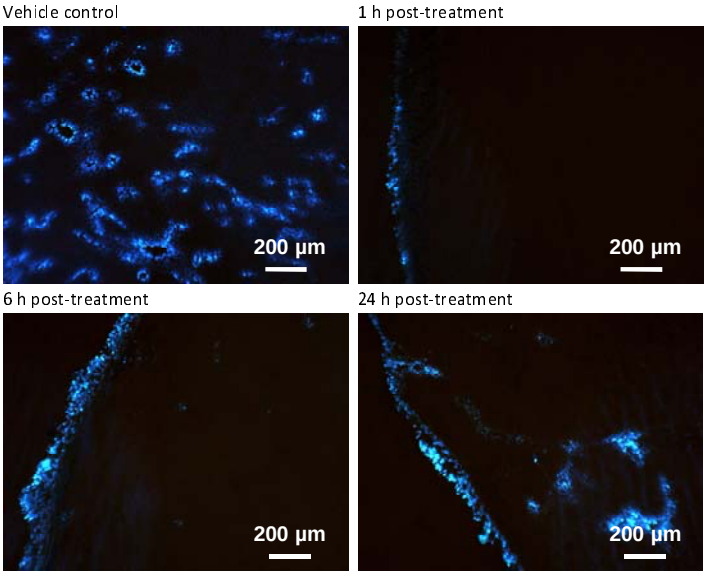

C